Filled tetrahedral semiconductor Li_3AlN_2 studied with optical absorption: Application of the interstitial insertion rule

K. Kushida,* Y. Kaneko, and K. Kuriyama†
College of Engineering and Research Center of Ion Beam Technology, Hosei University, Koganei, Tokyo 184-8584, Japan
(Received 12 March 2004; revised manuscript received 14 September 2004; published 3 December 2004)

The band gap nature of a *filled tetrahedral semiconductor* Li_3AlN_2 [viewed as the assemblage of eight hypothetical zinc-blende AlN sublattices $(Li_{0.5}Al_{0.5}N)^-$ filled with He-like Li^+ interstitials at the empty tetrahedral sites next to the anions] is studied by an optical absorption method. The optical absorption studies show a tendency that Li_3AlN_2 is *direct* with a band gap of 4.40 eV, whereas zinc-blende AlN has been estimated to be indirect from a first-principles calculation. The band gap value was confirmed by photoacoustic spectroscopy. According to the *interstitial insertion rule* of Wood *et al.*, these results suggest that the insertion of Li^+ ions into the interstitial sites in hypothetical zinc-blende AlN sublattices $(Li_{0.5}Al_{0.5}N)^-$ causes an upward shift of the X conduction band due to a Pauli repulsion of conduction electrons, exposing the Γ point as the conduction band minimum and resulting in a direct band gap.

DOI: 10.1103/PhysRevB.70.233303 PACS number(s): 78.40.Fy, 71.20.Nr, 78.20.Ci, 78.20.Hp

The band-structure modification of diamond and zinc-blende semiconductors has been theoretically tested by inserting small atoms such as H and He at their empty tetrahedral sites.[1–3] However, we encounter technological difficulties for the insertion. Instead of diamond and zinc-blende structures, Zunger's group[2,3] aimed at the ternary compounds $A^IB^{II}C^V$ (A^I=He like Li^+ ions, B^{II}=Zn or Mg, and C^V=As, P, or N), which have been originally classified into the Nowotny-Juza compounds.[4,5] They particularly referred the ternary $A^IB^{II}C^V$ as "filled tetrahedral compounds."[2,3] According to the *interstitial insertion rule* by Wood *et al.*,[2] the insertion of A^I (=Li^+ ions) interstitials into the empty tetrahedral sites next to the anions C^V in hypothetical III-V zinc-blende $(B^{II}C^V)^-$ causes an upward shift of the X point of the conduction band because of a Pauli repulsion between conduction electrons, which exposes the Γ as the conduction band minimum and converts indirect into direct band gap materials. In the previous studies, we synthesized LiZnX and LiMgX (X=N, P, and As) and found that these materials were all direct, supporting the interstitial insertion rule.[6–13]

Li_3AlN_2 is a Nowotony-Juza compound,[4,5] and its crystal structure depicted by Juza *et al.* is shown in Fig. 1(a). All atoms in the unit cell of Li_3AlN_2 are placed in the manner of preserving the inversion symmetry operation concerned with the body-centered N atom. On the other hand, Li_3AlN_2 has another representation of the unit cell, as shown in Fig. 1(b). The alternative unit cell includes eight small cubes drawn by solid lines instead of the dashed lined cubes. For a clear understanding, it would be better to divide the alternative unit cell of Li_3AlN_2 into the eight sublattices, one of which is shown in Fig. 1(c). It is considered that in each sublattice, 50% of Al atoms in zinc-blende AlN are substituted with Li. Therefore, each sublattice can be viewed as a zinc-blende-like $(Li_{0.5}Al_{0.5}N)^-$ filled with Li^+ at the empty tetrahedral sites next to N atoms. As shown in Fig. 1(c), two Al atoms are placed at the corners on only one side, which means the loss of symmetry demanded by the space group $F4\text{-}3m$ of the filled tetrahedral structure. However, in the unit cell, all atoms possess the 180° rotation symmetry around the z axis as shown in Fig. 1(b), resulting in space group[4,5] $Ia3$. Accordingly, Li_3AlN_2 consisting of the eight hypothetical zinc-blende sublattices leads to a filled tetrahedral semiconductor. Although the band gap nature of zinc-blende AlN has been estimated to be indirect with ~5.1 eV from a first-principles calculation,[14] we expect that the interstitial insertion rule can be applied to Li_3AlN_2. The synthesis and crystal data of Li_3AlN_2 have been already reported by Juza *et al.*[4] However, the optical band gap of Li_3AlN_2 has not been experimentally investigated. In this paper, we examine by an optical absorption method that insertion of Li^+ into the interstitial sites of AlN-like $(Li_{0.5}Al_{0.5}N)^-$ leads to a direct band gap nature.

Li_3AlN_2 crystals were synthesized by direct reaction between Li_3N (powder, 99.5% pure) and Al (wire, 99.999% pure) with the molar ratio Li_3N: Al of 1:1. A typical reaction temperature was 750 °C and was kept for 5 h. As-grown polycrystalline bulk is a single phase of Li_3AlN_2 with lattice parameter 9.427 Å. The details of the crystal growth will be reported elsewhere.[15]

Optical absorption measurements were performed using a scanning spectrophotometer (Shimadzu UV-3101 PC) at room temperature. This method was used for the measurements of the optical band gap of various tetrahedral semiconductors[7–13] and $LiInO_2$.[16] In the spectrophotometer used in the present study, the intensity of the light source (a halogen lamp) and the sensitivities of the monochromator and the detector are automatically calibrated over the wavelength range 250–800 nm to guarantee the linearity of the experimental setup. Figure 2 shows typical optical transmission spectra for the samples with the different thickness of 112 μm and 173 μm as a function of wavelength. The transmission curve for the 112-μm-thick sample showed an abrupt change at 400 nm (3.10 eV) and decreased down to 275 nm (4.51 eV). This result suggests that the absorption edge of Li_3AlN_2 lies between 3.10 and 4.51 eV.

Figure 3 shows three types of plot for the relationship between an optical energy ($h\nu$) and absorption coefficient (α) to more quantitatively test the band gap nature. The ab-

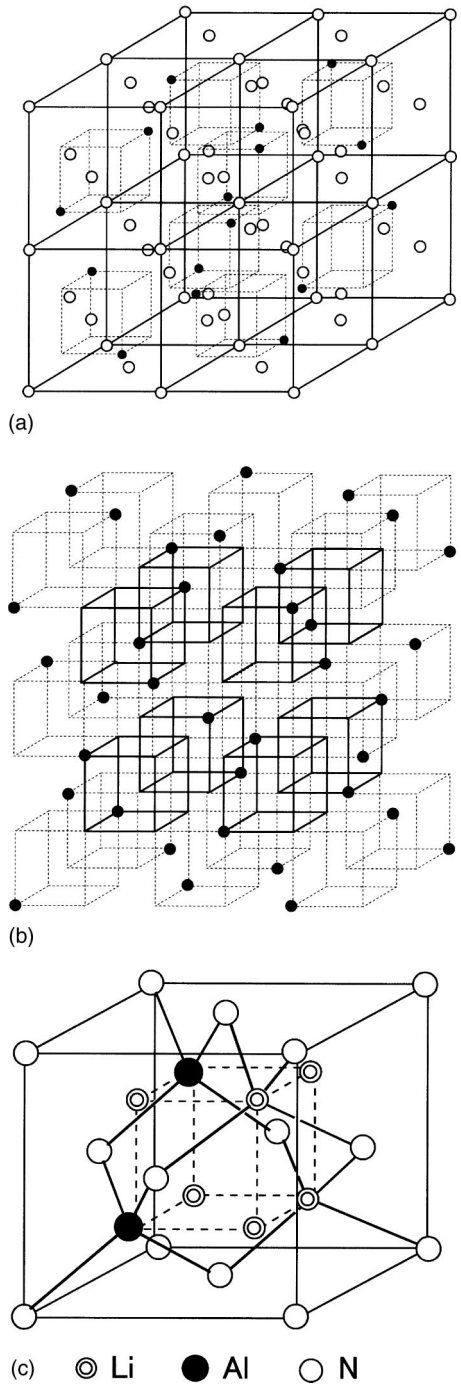

FIG. 1. (a) Crystal structure of Li_3AlN_2 (the space group $Ia3$) depicted by Juza *et al.* (Refs. 4 and 5). White circles=N, black circles=Al. Li atoms are not shown for clarity. (b) Another representation for the unit cell. (c) A sublattice in the alternative unit cell.

sorption coefficient can be calculated from the transmission spectra (T) experimentally obtained. The transmission spectra are formulated as follows:

$$T \sim I/I_0(1-R)^2\exp(-\alpha t),$$

where I is the transmitted light intensity, I_0 the incident light intensity, t the sample thickness, and R the reflectivity.[17] By

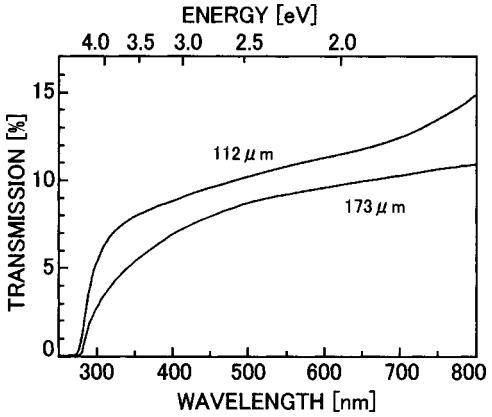

FIG. 2. Typical transmission spectra of Li_3AlN_2 at room temperature for different thickness of 112 and 173 μm.

using the transmission spectra of the two samples with different thickness t_1 and t_2 from the same batch, the unknown R is eliminated and the following relation[17] is obtained:

$$\alpha = [1/(t_1 - t_2)]\ln[T_1/T_2].$$

In the present study, the absorption coefficient was calculated using the transmission spectra of 112-μm- and 173-μm-thick samples as shown in Fig. 2. In general, the relation between $\alpha h\nu$ and $h\nu$ is formulated on the basis of

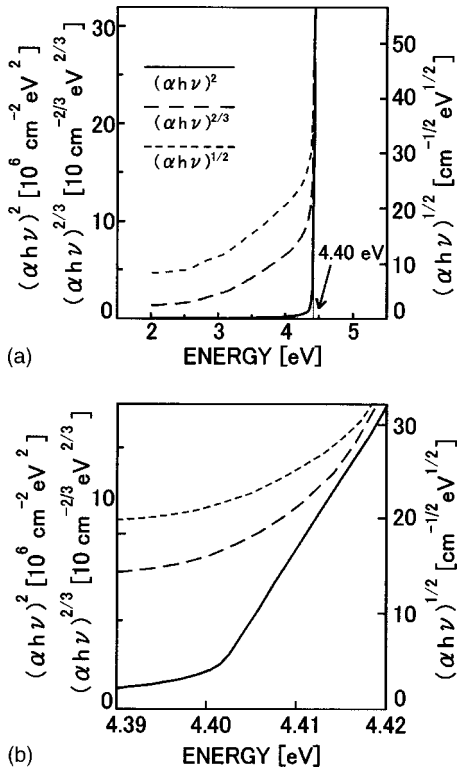

FIG. 3. (a) Plots to test three relations $(\alpha h\nu)^2$ vs $h\nu$ (solid line), $(\alpha h\nu)^{2/3}$ vs $h\nu$ (dashed line), and $(\alpha h\nu)^{1/2}$ vs $h\nu$ (shorter dashed line) for Li_3AlN_2 at room temperature. (b) The magnification of the critical regions of these three plots near the fundamental absorption edge.

the band gap nature as follows: $\alpha h\nu = A(h\nu - E_g)^{1/2}$ for allowed direct transitions at $\mathbf{k}=0$, $\alpha h\nu = A'(h\nu - E_g)^{3/2}$ for forbidden direct transitions allowed at $\mathbf{k}\neq 0$ or $\alpha h\nu = B(h\nu - E_g)^2$ for indirect transitions, where $\alpha h\nu$ is the product of α and $h\nu$, and E_g the energy gap.[17] In Fig. 3(a), we plotted $(\alpha h\nu)^2$, $(\alpha h\nu)^{2/3}$, and $(\alpha h\nu)^{1/2}$ against $h\nu$ using the experimentally obtained α, in order to examine the band gap nature of Li_3AlN_2 by comparing the linearity of these three curves (Refs. 7–12 and 16). The magnification of these three plots near the absorption edge (the critical regions) is also shown in Fig. 3(b). In these figures, solid line represents $(\alpha h\nu)^2$ vs $h\nu$, dashed line $(\alpha h\nu)^{2/3}$ vs $h\nu$ and shorter dashed line $(\alpha h\nu)^{1/2}$ vs $h\nu$ plots. The left-hand y axis is used to show both the $(\alpha h\nu)^2$ and $(\alpha h\nu)^{2/3}$, and the right-hand y axis is for the $(\alpha h\nu)^{1/2}$. If the band gap nature of Li_3AlN_2 is direct, the $(\alpha h\nu)^2$ vs $h\nu$ plot would hold linearity beyond the band gap according to the above formula and is expected to show better linearity near the absorption edge in comparison with the other two plots. In the critical region, the curve for the allowed direct transitions abruptly increased with high linearity, while the curves for indirect and forbidden direct transitions showed a gradual increase with a long tail near the absorption edge. Therefore, we believe that absorption data obey the relation of directness rather than that of indirectness (Refs. 7–12 and 16). When the linear portion of the plot is extrapolated to $\alpha=0$, the direct band gap E_g is estimated to be about 4.40 eV. These results indicate that when Li^+ ions are inserted into the empty tetrahedral sites next to N of each hypothetical zinc-blende lattice $(Li_{0.5}Al_{0.5}N)^-$, the X conduction band is shifted to higher energies in comparison with the other bands, exposing the Γ point as the conduction band minimum as predicted by the "interstitial insertion rule." The direct wide-band-gap nature of Li_3AlN_2 might result in various potential applications such as light emitting devices for the ultraviolet region. Furthermore, it would be advantageous that Li_3AlN_2 based on III-V zinc-blende structure has a cubic structure, while III-V materials with a direct wide band gap such as GaN or AlN normally crystallize in wurtzite (hexagonal) structure. The band gap of Li_3AlN_2 is relatively smaller than zinc-blende AlN ($\sim$5.1 eV),[14] which is consistent with the empirical tendency that the band gaps of other filled tetrahedral semiconductors such as LiZnP (E_g $\sim$2.04 eV),[7] LiZnN (1.91 eV),[8,10] LiMgN (3.2 eV),[12] and LiMgP (2.4 eV),[9] except for LiZnAs (1.51 eV),[13] were reduced by 10%–20% relative to their original zinc-blende materials (GaP, zinc-blende GaN and AlN, AlP). According to the bonding character of semiconductors described by Phillips,[18] since the zinc-blende III-V materials are coordinated fourfold, the total energy gap $E_g(=E_h+iC)$ is determined principally by a III-V bond, where E_h represents the average energy gap produced by a potential V_{covalent}, C the magnitude of the energy gap produced by a potential V_{ionic}, and i an imaginary number. Since each filled tetrahedral sublattice ($LiLi_{0.5}Al_{0.5}N$) is coordinated eightfold with six I and two II nearest neighbors [see Fig. 1(c)], the band gap of Li_3AlN_2 is associated with the bonding character of two kinds of the bonds: namely, Li-N and Al-N bonds. For wurtzite AlN, E_h and C are 8.17 and 7.30 eV, respectively, corresponding to the ionicity $f_i=0.449$ (Ref. 18). This implies that covalent bonds are preferable in AlN. According to Juza *et al.*,[4,5] the Al-N bond distances are about 12% smaller than the distances from the N atoms to the other tetrahedral sites, suggesting that the covalency of Al-N bonds increases because of the enhancement of the orbital overlap of wave functions between Al and N. Therefore, it is suggested that the relatively small band gap of Li_3AlN_2 in comparison with zinc-blende AlN is attributed to the relatively high covalency of Al-N bonds exceeding the ionicity of Li-N bonds to keep the cubic phase without a phase transition to wurtzite structure. On the other hand, the optical band gap of Li_3AlN_2 is larger than the band gap (3.2 eV) of an AlN-like filled tetrahedral semiconductor LiMgN [He-like Li^+ ions plus hypothetical zincblende $(MgN)^-$].[12] This means that the relatively high ionicity of Li-N bonds exceeding the covalency of Mg-N is introduced into Li_3AlN_2 by replacing 50% of Al in zinc-blende AlN with a lighter element Li.

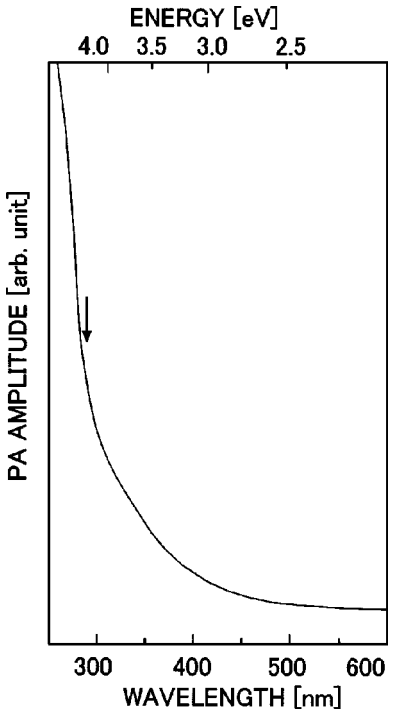

FIG. 4. A photoacoustic emission spectrum for Li_3AlN_2 at room temperature. The energy position corresponding to the optical band gap (4.40 eV) is indicated by an arrow.

Photoacoustic spectroscopy (PAS) was employed to confirm the band gap value (4.40 eV) measured by the optical absorption. A detailed configuration of the PAS measurement will be reported elsewhere.[15] A photoaoustic signal is related to the nonradiative part of deexcitation or recombination in materials. Figure 4 shows PAS spectrum for Li_3AlN_2. The PA signal of Li_3AlN_2 began to increase at $\sim$400 nm ($\sim$3.1 eV) and was abruptly enhanced around $\sim$280 nm ($\sim$4.4 eV). This abrupt enhancement would be mainly attributed to the nonradiative process of excited carriers arising from the absorption of photon energy, corresponding to the band gap of Li_3AlN_2. The evaluated gap value supports the optical band gap (4.40 eV).

In conclusion, the optical absorption studies showed a tendency that Li_3AlN_2 is *direct* with a forbidden gap of 4.40 eV. The band gap value was supported by photoacoustic spectroscopy. This result suggests that insertion of Li^+ into the interstitial sites in zinc-blende-like $(Li_{0.5}Al_{0.5}N)^-$ lattices causes a direct band gap because of an upward shift of the *X* point in Brillouin zone. Further advanced studies of the band gap nature by other methods such as ellipsometry and photoluminescence techniques will be reported, when the single crystals are obtained in the near future. Li_3AlN_2 is a new type of filled tetrahedral semiconductor that follows the "interstitial insertion rule."

The present work was supported in part by a Grant-in-Aid for Scientific Research on Basic Areas from the Japanese Ministry of Education, Culture, Sports, Science and Technology (No.15360014) and also supported by the Yazaki Memorial Foundation for Science and Technology. The authors would like to thank Hiroyasu Nakata of Osaka Kyoiku University for the use of a photoacoustic spectroscopy instrument.

---

*Present address: Department of Arts and Sciences, Osaka Kyoiku University, Kashiwara, Osaka 582-8582, Japan.
†Corresponding author. Email address: kuri@ionbeam.hosei.ac.jp

[1] H. W. M. Rompa, M. F. H. Schuurmans, and F. Williams, Phys. Rev. Lett. **52**, 675 (1984).
[2] D. M. Wood, A. Zunger, and R. de Grood, Phys. Rev. B **31**, 2570 (1985).
[3] A. E. Carlsson, A. Zunger, and D. M. Wood, Phys. Rev. B **32**, 1386 (1985).
[4] R. Juza and F. Hund, Z. Anorg. Chem. **257**, 13 (1948).
[5] R. Juza, K. Langer, and K. V. Benda, Angew. Chem., Int. Ed. Engl. **7**, 360 (1968).
[6] R. Bacewicz and T. F. Císzek, Appl. Phys. Lett. **52**, 1150 (1988).
[7] K. Kuriyama and T. Katoh, Phys. Rev. B **37**, 7140 (1988).
[8] K. Kuriyama, T. Katoh, and T. Tanaka, Phys. Rev. B **49**, 4511 (1994).
[9] K. Kuriyama, K. Kushida, and R. Taguchi, Solid State Commun. **108**, 429 (1998); in *Proceedings of the 24th International Conference on the Physics of Semiconductors, Jerusalem, 1998*, edited by D. Gershoni (World Scientific, Singapore, 1999), CD-ROM No. 0229.
[10] K. Kuriyama, R. Taguchi, K. Kushida, and K. Ushiyama, J. Cryst. Growth **198/199**, 802 (1999).
[11] K. Kuriyama and K. Kushida, J. Appl. Phys. **87**, 3168 (2000).
[12] K. Kuriyama, K. Nagasawa, and K. Kushida, J. Cryst. Growth **237/239**, 2019 (2002).
[13] K. Kuriyama, T. Kato, and K. Kawada, Phys. Rev. B **49**, 11 452 (1994).
[14] W. R. L. Lambrecht and B. Segall, Phys. Rev. B **43**, 7070 (1991).
[15] K. Kuriyama, Y. Kaneko, and K. Kushida, J. Cryst. Growth (to be published).
[16] K. Kushida, T. Koba, and K. Kuriyama, J. Appl. Phys. **93**, 2691 (2003).
[17] J. I. Pankov, *Optical Processes in Semiconductors* (Dover, New York, 1975), Chap. 3.
[18] J. C. Phillips, *Bonds and Bands in Semiconductor* (Academic, New York, 1973), Chap. 2.